Multiphoton ionization of rare gases by a tunable-wavelength 30-psec laser pulse at 1.06 μm

L. A. Lompre, G. Mainfray, C. Manus, and J. Thebault
Service de Physique Atomique, Centre d'Etudes Nucléaires de Saclay, BP No. 2-91190 Gif-Sur-Yvette, France
(Received 30 August 1976)

Multiphoton ionization of xenon, krypton, and argon atoms has been investigated by using a tunable-wavelength bandwidth-limited 30-psec laser pulse of 10^{13} W/cm^2 at 1.06 μm. The laser linewidth is 0.8 cm^{-1}, and the laser wavelength can be tuned over a range of 80 Å. No resonant effects have been observed within this wavelength range, although resonance conditions are satisfied. The absence of resonance effects could be explained in terms of the short laser pulse duration. Laser light polarization effects were still measured. Moreover, the ionization energy of krypton has been observed to be lowered by 86 ± 6 cm^{-1} under the influence of a laser electric field of 1.2×10^8 V cm^{-1}.

I. INTRODUCTION

Multiphoton ionization processes have been the subject of a considerable number of recent experimental works,[1-13] and the general rules governing such processes have now become apparent. Multiphoton ionization of atoms emphasizes both atomic properties and laser properties, namely frequency, coherence, and polarization. But the role played by each of these parameters varies with the number of photons involved in the ionization process. For example, the statistical properties of a laser pulse are not significant in the two-photon ionization of alkali-metal atoms at fairly low intensity (10^7 W/cm^2), whereas they become the dominant factor in higher-order ionization processes,[14-19] such as the ionization of rare gases with a 1.06-μm laser pulse at very high intensities (10^{13}–10^{15} W/cm^2).

Although the situation is not yet as clear for resonant effects, it is known that the shape of a resonant multiphoton ionization profile is governed by a larger number of parameters: laser intensity, pulse shape and duration, temporal coherence, and such intensity-dependent atomic parameters as the widths and shifts of both the ground state and the intermediate resonant state. The multiphoton ionization rate of an atom, as a function of the laser frequency, exhibits a typical resonant character when the energy of an integer number of photons is close to the energy of an atomic level satisfying the parity selection rule. Thus, a resonant enhancement of five orders of magnitude in the four-photon ionization rate of cesium has been observed by using a single-mode, tunable-wavelength, Q-switched Nd-glass laser at intensities of 10^8–10^9 W/cm^2.[20] Although resonant multiphoton ionization experiments have been carried out with cw or with long pulses from Q-switched lasers (10^{-8} sec), resonant processes have not yet been studied utilizing very short laser pulses (10^{-11} sec).

In a previous experiment,[21] multiphoton ionization of rare gases was investigated by using a 30-psec laser pulse from a mode-locked Nd-YAG oscillator at fixed frequency. The experimental results seemed to indicate that no resonant processes had taken place. Previous experiments using 10^{-8}-sec laser pulses have shown that resonant multiphoton ionization processes in rare gases do exist and are characterized by both an enhancement of the ionization rate W, and a significant variation of the slope $K = \partial \ln W / \partial \ln I$, as a function of the laser frequency, where I is the laser intensity.[20,22-24]

The purpose of the present work was to investigate further whether or not resonant multiphoton ionization of rare gases was still observable on the 10^{-11}-sec time scale. For this purpose, a tunable-wavelength mode-locked Nd-glass laser was used. It was tunable over a range of 80 Å, with temporal and spectral characteristics similar to a mode locked Nd-YAG laser. It should be pointed out that measurements using such ultrashort laser pulses must be undertaken with extreme care in order to avoid misleading inferences from the experimental results. In particular, it was necessary to record carefully all the pulse parameters from each laser shot.

II. EXPERIMENTAL METHOD

A. Tunable-wavelength mode-locked Nd-glass oscillator

The temporal and spectral characteristics of the output from a mode-locked Nd-glass laser have been the subject of many investigations. It is well known that several deviations from perfect mode-locking have been observed in passively mode-locked lasers. The shape and duration of

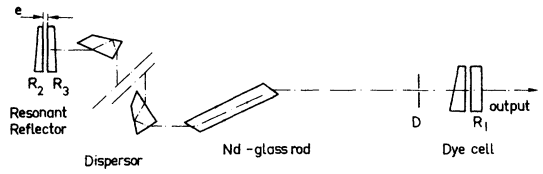

FIG. 1. Scheme of the tunable-wavelength mode-locked Nd-glass oscillator. D-circular aperture; the dispersor is a prism array which consists of eight Brewster angle Abbe prisms. Mirror reflection coefficient $R_1=R_2=R_3=0.65$. The thickness of the Fabry-Perot $e=0.3$ mm.

the individual pulses vary throughout the pulse train. At the beginning of the pulse train, the pulses have a smooth shape, and are transform-limited with 5-psec duration. The more complex pulses observed later in the train, however, possess a definite structure, have a total duration of 20–50 psec, and exhibit a strong frequency modulation.[25]

In order to generate reproducible 30-psec pulses, the laser bandwidth is narrowed by putting eight highly dispersive Abbe prisms and a resonant reflector in the cavity. Because only a small fraction of the bandwidth is used for mode locking, frequency tuning of the pulses is thus possible.

Although this novel laser is described in detail elsewhere,[26] a brief description will be given here. Figure 1 shows the main elements of the oscillator. The Owen-Illinois ED-2 laser rod is 200 mm long, 16 mm in diameter, and Brewster ended. Mode locking is achieved by using Kodak 9740 saturable dye. This dye is in liquid contact with the output mirror which has a reflection coefficient $R_1=0.65$. Transverse mode selection is made with a pinhole D. In the absence of selective elements in the oscillator, the total width of the emission spectrum is 15 Å. When the prism array is used as the selector, the spectrum can be reduced to a width of 5 Å. When the prism array and Fabry-Perot etalon are used simultaneously, the laser emission spectrum is reduced to a width of 0.8 Å. Each of the eight Brewster angle Abbe prisms that constitute the prism array gives a 90° deviation of the incident beam at maximum dispersion. Also each prism is cut and oriented in such a way that the incident and emerging beams always enter and exit at the Brewster angle to minimize losses, and to linearly polarize the laser light. The dispersion is additive for all prisms, so that the total angular dispersion is $\partial\theta/\partial\lambda=9\times10^{-5}$ rad Å^{-1}. The Fabry-Perot etalon works in reflection. It consists of two mirrors which have nearly the same reflection coefficient ($R_2=R_3=0.65$) and are separated by 0.3 mm. It has a finesse of eight. The adjustment of the optical elements in the laser cavity is easily obtained by using a cw YAG laser. Wavelength tuning is achieved over the range of 10 580–10 660 Å by changing the angle of inclination of the etalon with respect to the laser cavity axis. This oscillator, which produces a smoothly varying pulse train 600 nsec in length and individual pulses separated by 15 nsec, possesses a very good long-term stability.

B. General experimental arrangements

By using a Pockels switch, a single pulse was selected from the early part of the pulse train generated by the mode-locked Nd-glass oscillator. This single pulse, typically having an energy of ~0.1 mJ, is amplified by two Nd-glass preamplifiers to an energy of ~1 mJ and then traverses a beam expanding telescope before entering a three-stage Nd-glass amplifier. The single pulse can thus be amplified to an energy up to 1 J. Multiphoton ionization of argon, krypton, and xenon atoms is performed by using an arrangement identical to that employed in our previous experiments.[14] Figure 2 shows a schematic diagram of the experimental arrangement. Briefly, the laser pulse is focused into a vacuum chamber by an $\frac{1}{3}f$ aspheric lens corrected for spherical aberrations. The laser intensity used in the focal region is about 10^{13} W/cm^2. The laser pulse energy is measured by using a photodiode which was calibrated by comparison with a TRG calorimeter. The gas under investigation is released into the vacuum chamber at a static pressure of 10^{-4} Torr at which no avalanche effects occur. The ions, normally $10-10^4$ in number resulting from the interaction of the laser photons with the atoms at the focal volume are extracted with a transverse electric field of 300 V cm^{-1} and then detected with an electron multiplier.

The experiment consists of measuring the number of ions formed as a function of the laser intensity, for a given laser wavelength. In usual multiphoton ionization experiments with nsec laser pulses, the laser intensity is generally varied by inserting neutral density filters in the laser beam. This procedure, however, is not useful in the present experiment. As was shown in a previous work[21] with a mode-locked Nd-YAG laser, the effective surface of the focal volume, is slightly changed every time the laser power is intentionally varied. It should be pointed out that both lens aberrations and laser aberrations govern the focused intensity distribution. Lens aberrations were minimized in the present experiment by using a corrected aspheric lens. Laser aberrations,

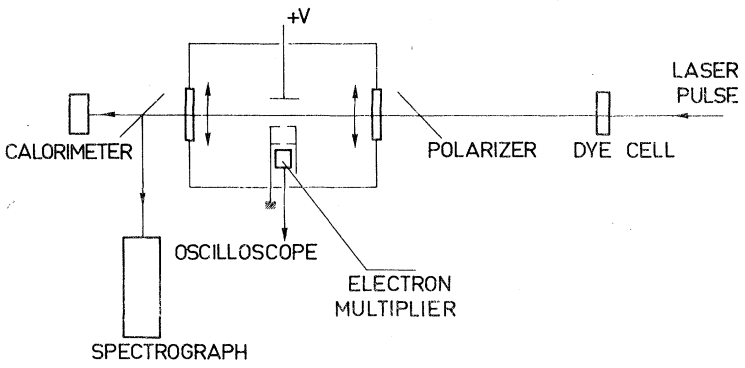

FIG. 2. Schematic diagram of the experimental setup.

which mainly govern the focused intensity distribution, can be modified by intentionally varying the laser power, but this can change the effective diameter of the focal region. We have used a different method more suitable for the present experiment. The laser power is not intentionally varied; instead, a dye cell (Kodak 9740 in chlorobenzene) is permanently placed in the path of the laser pulse, as shown in Fig. 2, to enhance the power fluctuations of the laser from shot to shot. These enhanced power fluctuations extending over an 80% range is enough to have a corresponding variation of the number of ions over three orders of magnitude. All the outstanding laser parameters were measured with the dye cell in the laser beam.

C. Diagnostics of a bandwidth-limited pulse

A bandwidth-limited pulse is defined as a pulse completely devoid of intensity and frequency modulation. It has a regular and well-defined temporal behavior, similar to a single-mode laser pulse. Since no fluctuation occurs, the Kth-order peak intensity autocorrelation function equals unity.[14,17,18] This makes the comparison easier between theoretical and experimental multiphoton ionization rates. Verification of bandwidth-limited operation requires that careful and detailed diagnostics be applied to each laser pulse in both the time and frequency domains.

1. Pulse duration

The beam-expanding telescope was adjusted to have a slightly diverging laser beam because of increasing diameter of successive amplifier rods. Compensation for the divergence of the amplified laser beam was achieved by placing a long focal length (4-m) lens in the laser beam after the dye cell. A fraction of the laser energy reflected from the plane face of this lens is optically delayed and is directed onto the entrance slit of a psec streak camera. The 5-psec resolution streak camera is of conventional design and has been described in detail elsewhere.[27] It consists of an image converter EEV-P855 having an S_1 photocathode, and is coupled by a lens with an EMI-9694 magnetically focused image intensifier. A beam splitter similar to a Michelson interferometer, put between the entrance slit and the photocathode of the streak tube, gives two spatially coincident images of the slit. The time calibration is obtained from the flight difference between the two pulses corresponding to a known difference of length between the two paths. Moreover, a neutral density filter (0.15 optical density at 1.06 μm), through which laser light passes twice, is put in one arm of the interferometer. Thus because one of the two pulses is more intense than the other by a factor of 2, the half maximum width calibration is easily obtained. Detection is achieved either on photographic film, or on a TV screen.[27] Figure 3(a) shows a typical densitometer trace of the streak photograph of a single pulse which has been split in the manner just discussed. The recorded pulse exhibits a smooth, time-symmetric dependence. The pulse width at half maximum measured to be 30 ± 2.5 psec, remains constant when the laser wavelength is tuned over a range of 80 Å.

2. Spectral distribution

Laser spectral emission of the amplified single pulse is analyzed by using a diffraction grating spectrograph which has a dispersion of 4 Å/mm and a resolution of 0.1 cm^{-1} at 1.06 μm. A neutral density filter (0.3 optical density at 1.06 μm) is placed in front of the entrance slit of the spectrograph to cover half of the height of the slit. Both halves are uniformly illuminated by the pulse. This device gives the half maximum width calibration. Figure 3(b) shows a typical densitometer trace of the laser linewidth. The pulse consists of a single spectral line which has a smooth, symmetric, and bell-shape behavior. The line-

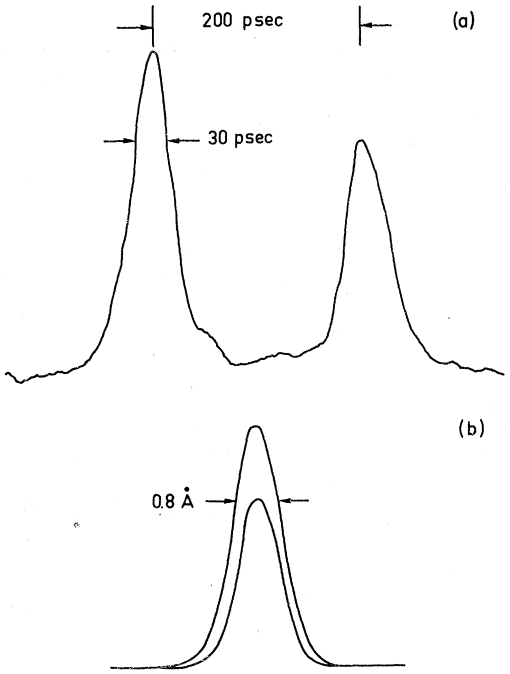

FIG. 3. (a) Typical densitometer trace of a streak photograph of a single pulse. Temporal scale is given by the pulse separation. The top of the smaller pulse determines FWHM light intensity level of the main pulse. (b) Typical densitometer trace of the spectral distribution of the laser intensity. The top of the smaller spectral line determines FWHM of the main spectral line.

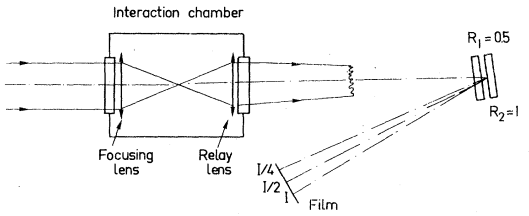

FIG. 4. Experimental setup for photographing the focal region. The relay lens projects a 40× magnified focal spot image onto the film. The partially reflecting mirror pair $R_1 - R_2$ provides known intensity ratios to the film.

width at half maximum measured as $\Delta\lambda = 0.8 \pm 0.05$ Å, remains constant when the laser wavelength is tuned over a range of 80 Å. In general, a bandwidth-limited pulse has a time-frequency product between 0.45 and 1, depending on the temporal and spectral distribution functions. For example, a bandwidth-limited pulse with strictly Gaussian temporal and spectral distributions has a time-frequency product of 0.45. For our laser, the corresponding time frequency product is $\Delta\nu \times \Delta t \simeq 0.75$. Thus the results of the temporal and spectral properties of the laser pulse are experimental confirmation that the laser pulse is indeed bandwidth limited.

D. Focused laser intensity measurements

The accuracy of the absolute laser intensity measurements in the focal region is mainly defined by the accuracy of the surface determinations of the focal volume. The focal region is reimaged with 40× magnification outside the interaction chamber and photographed on a film. Figure 4 shows the experimental setup. These measurements, performed with a pressure of 10^{-4} Torr in the interaction chamber, are made with the same laser power as used in taking the multiphoton ionization data. The focal volume measurements are carried out with the dye cell placed in the laser beam. To keep the response of the photographic film in the nonsaturated region, when exposed to the laser, a partially reflecting mirror pair is used to provide known intensity ratios. Isodensitometer processing of film images then gives the laser intensity in different planes near the focus. Figure 5(a) shows the isodensity contours in the plane corresponding to the smallest surface, and Fig. 5(b) shows the sectional elevation densitometer trace along the XY axis. The focal spot diameter is measured to be 15 ± 3 μm.

These measurements have been completed by

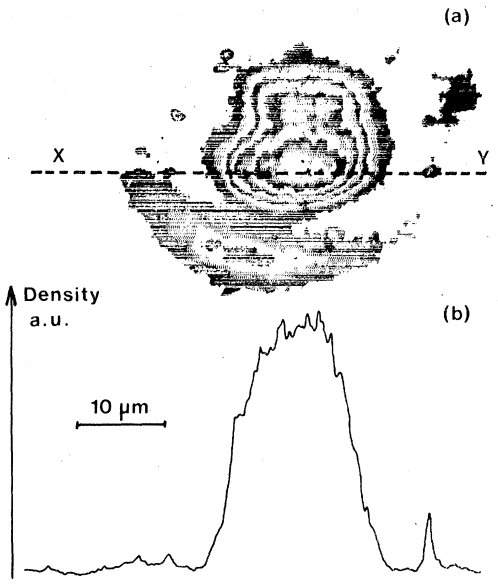

FIG. 5. (a) Isodensity contours obtained by isodensitometer processing of film image for the best focal plane. (b) Sectional elevation densitometer trace along the XY axis.

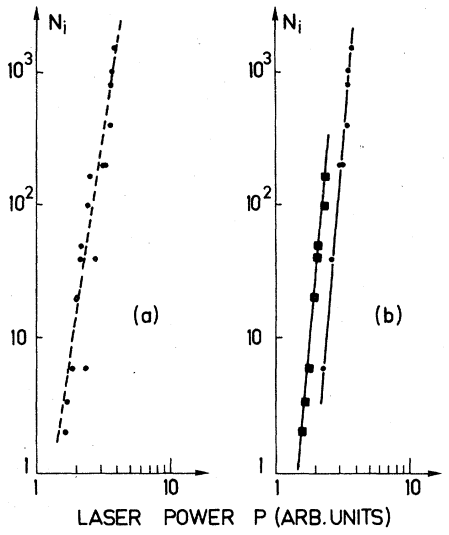

FIG. 6. Log-log plot of the variation of the number of xenon ions N_i as a function of the laser power P. The laser wavelength in vacuum is 10 644 Å. (a) The rough results give an apparent slope $K = \partial \ln N_i / \partial \ln P \simeq 7$, with large scattering in experimental points. (b) The same ion data when experimental points are classified according to the intensity and position of the single pulse selected in the mode-locked train in accordance with Fig. 7. The measured slope is then $K = 11$.

time-resolved focal measurements. The 200× magnified image of the focal spot is projected onto the slit of the 5-psec resolution streak camera. No distortion is observed, either in the laser pulse or in the focal spot. This result is in agreement with another experiment,[28] in which a spreading of the focal region was observed only when the laser power was larger than 100 GW, and characterized by B values larger than 3. The break-up integral B is the integrated gain of the most unstable spatial frequency along the path length l, and is defined by

$$B = \int g \, dl, \tag{1}$$

where g is the gain coefficient for the most unstable spatial frequency. In the present experiment, B, which is considered as a useful parameter to characterize the focusing properties of a laser pulse has been estimated to be less than 0.4 for the maximum available power.

III. EXPERIMENTAL RESULTS AND DISCUSSION

A. Preliminary remarks

Figure 6(a) shows on a log-log plot the number of ions N_i as a function of the laser power P, for xenon atoms. The large scattering of experimental points observed is inconsistent with the use of bandwidth-limited pulse.[14] Moreover, the apparent slope is $K = \partial \ln N_i / \partial \ln P \simeq 7$, which is much less than K_0, defined as the next integer greater than the ionization energy of the atom divided by the laser photon energy. For xenon, the expected value is $K_0 = 11$. As a matter of fact, this rough result can be misleading, so the following remarks should be made. A single pulse is selected from the early part of the pulse train generated by the mode-locked oscillator. The trigger level of the Pockels switch is set at a definite power in the very early part of the laser pulse train where two successive pulses have nearly the same intensity. The delay time between the triggering laser pulse and the selected pulse is about 20 nsec. A jitter of one pulse in the triggering is possible from shot to shot. Hence, it follows that a jitter of one pulse can take place in the single selected pulse. Figure 7 is a schematic oscilloscope trace showing the early part of the pulse train generated by the mode-locked oscillator with one single selected pulse missing. Figures 7(a) and 7(b) correspond to two possible cases. Δt and $\Delta \nu$ have been verified to be the same for both cases, but the two selected pulses in the figure have a different intensity. According to a previous work,[21] as well as the remarks in Sec. II B, the effective surface of the focal volume can be slightly different for each case in Fig. 7. This difference in the effective surface has to be taken into account in the rought result shown in Fig. 6(a), because the number of ions formed is very sensitive to the varia-

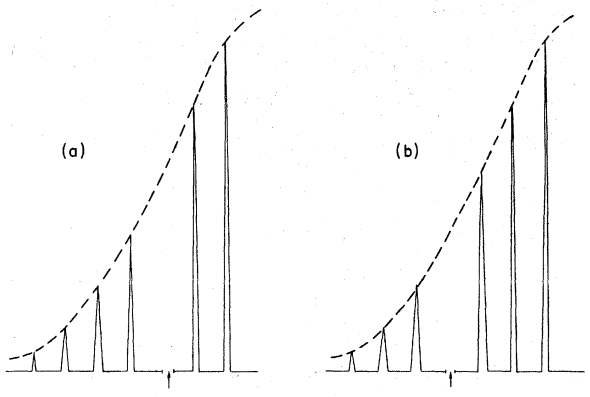

FIG. 7. Schematic oscilloscope trace showing the early part of the pulse train generated by the mode-locked oscillator, with one single selected pulse missing. (a) and (b) correspond to two different cases with different intensity in the single selected pulse due to different position in the pulse train. The arrow shows the position of the single selected pulse in both cases.

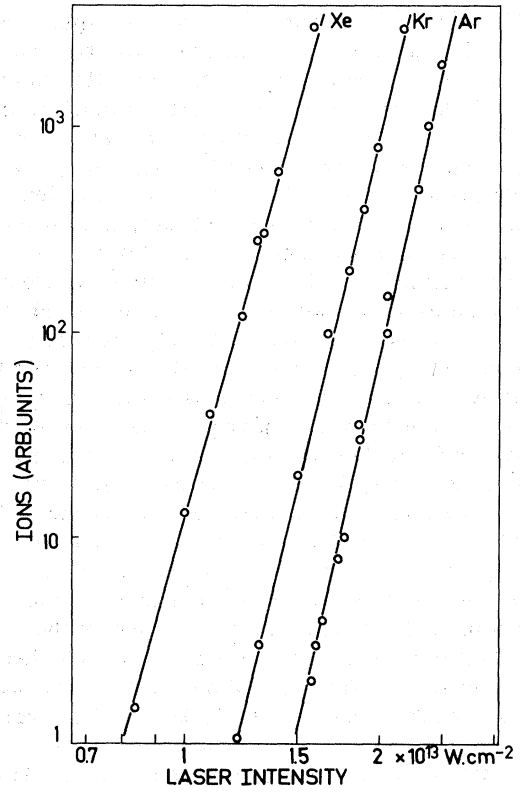

FIG. 8. Log-log plot of the variation of the number of ions formed N_i as a function of the laser intensity I for xenon, krypton, and argon atoms. The laser wavelength in vacuum is 10 644 Å. An expanded scale is used in the laser intensity axis to obtain a better accuracy in the slope $K = \partial \ln N_i / \partial \ln I$; $K = 11 \pm 0.2$ for Xe, $K = 13 \pm 0.2$ for Kr, and $K = 14 \pm 0.2$ for Ar.

tion of the laser intensity due to a small difference in the effective surface of the focal volume. Figure 6(b) shows ion data after the experimental points have been classified in connection with case 7(a) and 7(b). The experimental points then fall on two parallel straight lines which have the same slope, $K = 11$. Later on, we shall deal with experimental results obtained with the same single selected pulse, the intensity of which is defined according to the preceding pulse in the train.

Figure 8 shows, on a log-log plot, the experimental results obtained for multiphoton ionization of xenon, krypton, and argon atoms, when the laser wavelength is 10 644 Å in vacuum. To get a more accurate value of the slope, $K = \partial \ln N_i / \partial \ln I$, experimental results are displayed on an expanded logarithmic scale along the laser intensity axis, to emphasize the alignment and lack of scattering in the data. This is expected when bandwidth-limited pulses are used, because the Kth-order peak intensity autocorrelation function equals unity, as shown in a previous paper which investigated the influence of the statistical properties of a laser pulse on multiphoton ionization processes.[14]

B. Disappearance of resonance effects

The laser wavelength was tuned over a range of 80 Å, from 10 660 to 10 580 Å, by steps of 3 Å. For each laser wavelength, a log-log plot of the number of ions formed as a function of the laser intensity was obtained. For a given laser intensity, experimental results obtained with xenon and argon atoms show that: (i) The number of ions formed remains the same, within experimental errors, when the laser wavelength is tuned over a range of 80 Å, and (ii) The slope K remains constant and equal to K_0 when the laser wavelength is tuned over a range of 80 Å. $K = 11 \pm 0.2$ for xenon atoms, and $K = 14 \pm 0.2$ for argon atoms.

The results give no evidence of resonance effects, although resonant multiphoton excitation of several atomic levels satisfying the parity selection rule is possible. For example, resonant 13-photon excitation of $7s$ or $5d$ states should be possible in argon atoms, as shown in Fig. 9, a schematic energy diagram of argon in the energy range near that of 13 laser photons. The energy of 13 photons is varied from 122 000 to 122 750 cm^{-1} when the laser wavelength is tuned over a range of 80 Å. Thus resonant conditions are satisfied, but no resonance effect has been experimentally observed. At first sight, it may be thought that the 0.8-cm^{-1} linewidth of the 30-psec laser pulse is a damping term large enough to completely damp resonance effects. However, in a previous experiment,[23] resonance effects in 11-photon ionization of xenon atoms have been clearly observed in the same wavelength region with 10^{-8}-sec laser pulses and with a laser linewidth of about 1 cm^{-1}. This is an indication that the laser linewidth itself is not the most relevant parameter.

A more likely explanation of the disappearance of resonances in the present work is to be found in the comparison of the short duration (10^{-11} sec) of the laser pulse here with respect to the 10^{-8} sec interaction time in previous experiments.[5,6,20,22,23] It should be recalled that multiphoton ionization near a resonance is described in the following way: (i) a direct nonresonant K_0-photon absorption process, and (ii) a p-photon transition from the ground state to a quasiresonant state, followed by a one- or two-photon absorption from this quasiresonant state to a continuum state. The resonant transition channel

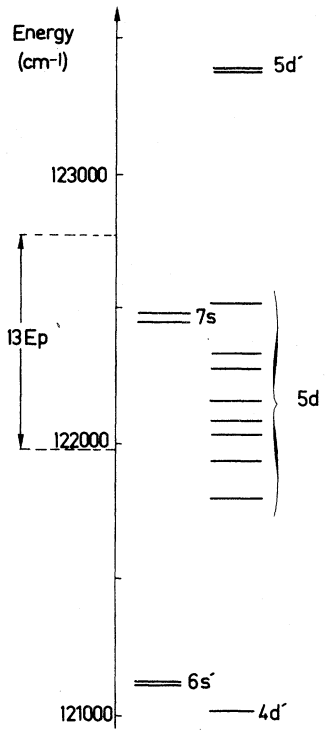

FIG. 9. Possible resonant 13-photon excitation of s or d states in argon atoms. The energy of 13 laser photons is varied from 122 000 to 122 750 cm^{-1} when the laser wavelength is tuned over a range of 80 Å. Direct multiphoton ionization of argon results from simultaneous absorption of 14 photons.

takes a much longer time to occur than the nonresonant process.

When a very short laser pulse is used, it can be expected that the resonant process does not have enough time to take place during the laser pulse duration. Thus, when the laser pulses are shorter than the time required for a resonant process to occur the multiphoton ionization process would be governed only by the nonresonant process. This assumption is supported by a recent theoretical work,[29] a model using the density matrix formalism and a classical description of the laser field. This model is a method by which the influence of the characteristics of the laser pulse, the pulse shape, and especially the pulse duration, on the multiphoton ionization process may be studied. However, this model assumes that the resonant level is closer to the ground state than to the continuum, a condition that is not fulfilled in rare gases. Consequently, this model cannot be directly applied to the present work, and no comparison is made here.

The hypothesis that the disappearance of resonances is due to the short pulse duration will be tested in the near future by using the tunable-wavelength 30-psec laser pulse to investigate the four-photon ionization of cesium atoms at a laser intensity of 10^9 W/cm^2. This interaction has been carefully described in 10^{-8}-sec time scale and gave evidence of a typical resonant character.[20]

C. Lowering of the ionization energy of krypton

An additional conclusion can be drawn from the experimental results for krypton. Multiphoton ionization of krypton is a special case when the laser wavelength is tuned between 10 600 and 10 650 Å as this energy range corresponds to a transition from a 12-photon to a 13-photon ionization process. This transition can be seen in Fig. 10, a graph of the slope K as a function of the laser frequency deduced from the laser wavelength in vacuum. The change of slope occurs at a laser frequency of 9402.5 ± 0.5 cm^{-1}. This indicates an ionization energy of $112\,829 \pm 6$ cm^{-1} as compared to the value of the ionization energy of krypton atoms taken from Moore's tables, 112 915 cm^{-1}. Thus it seems that the ionization energy of the krypton atom is lowered by 86 ± 6 cm^{-1} under the influence of the laser electric field $E = 1.2 \times 10^8$ V/cm. It should be emphasized that the measured shift of 86 cm^{-1} does correspond not only to a lowering of the continuum limit by 86 cm^{-1}, but to a difference in the shift of the ground state and the shift of the continuum limit of the atom.

A recent calculation has been performed to investigate the perturbation of atomic Rydberg states in the presence of a nonresonant laser light.[30] It was shown that all the Rydberg states are shifted by the same amount with respect to the ground state, but that the ground state generally under-

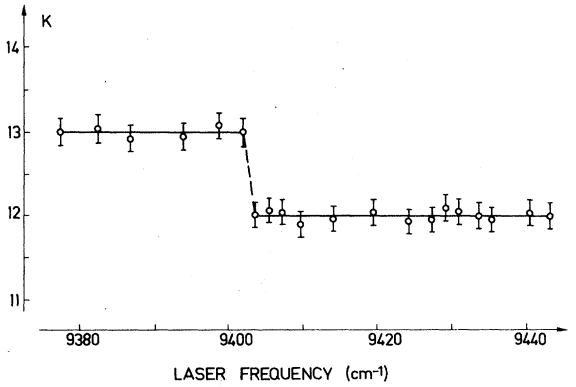

FIG. 10. Variation of the slope K for krypton atoms as a function of the laser frequency in cm^{-1} deduced from the laser wavelength in vacuum.

goes a different shift. However, this calculation cannot be applied to the high laser intensity values which are needed to investigate multiphoton ionization of rare gases at 1.06 μm.

D. Laser polarization effects

All the preceding experiments were performed with linearly polarized laser light. As is well known, the multiphonon ionization rate depends on the polarization of the laser light, through the selection rule on the magnetic quantum number. The preceding experiments were also performed with circularly polarized laser light. No resonant effects is observed when the laser wavelength was tuned over a range of 80 Å, when circularly polarized laser pulses are used. Figure 11 is a log-log plot of the number of krypton ions as a function of the laser intensity for linear and circular polarization. It can be seen that linear polarization is more efficient than circular polarization, in agreement with theoretical predictions.[31,32] The ratio between the 13-photon ionization rate of krypton for linearly and circularly polarized laser light is measured to be 70 ± 8. The same measurements have been carried out for xenon atoms. The ratio between the 11-photon ionization rate of xenon for linearly and circularly polarized laser light is measured to be 38 ± 6. This ratio remains constant when the laser wavelength is tuned over a range of 80 Å.

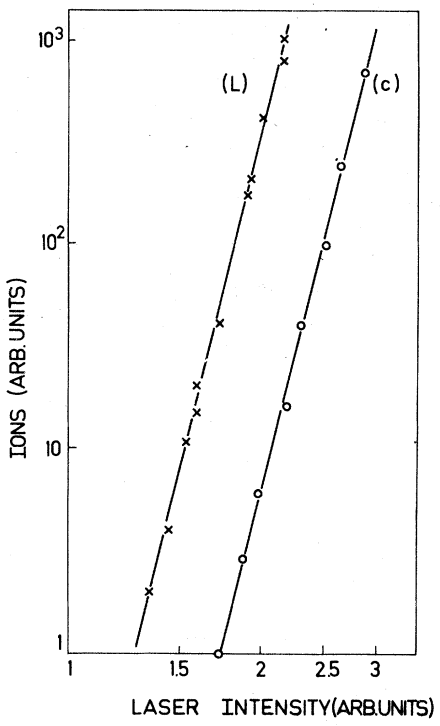

FIG. 11. Log-log plot of the variation of the number of krypton ions as a function of the laser intensity for linear (L) and circular (C) polarization of laser light. The laser wavelength in vacuum is 10 650 Å. An expanded scale is used in the laser intensity axis to obtain a better accuracy.

E. Multiphoton and tunneling effects

It has been shown by Keldysh[33] that the behavior of the multiphoton ionization is related to the parameter γ defined as

$$\gamma = (\omega/eE)(2mI_0)^{1/2}, \tag{2}$$

where ω and E are the angular frequency and peak electric field of the laser radiation, respectively. I_0 is the ionization energy of the atom, and e and m are the charge and mass of the electron, respectively. This parameter γ is generally considered as a characterization parameter between multiphoton process, $\gamma \gg 1$, and a tunneling effect, $\gamma \ll 1$. In a previous experiment,[21] multiphoton ionization of neon and helium was still observed at a laser intensity of 10^{15} W/cm^2 for which: $\gamma \simeq 0.35$. *A fortiori* in the present work, ionization of xenon, krypton and argon at a laser intensity of about 10^{13} W/cm^2 ($\gamma \simeq 2$) is expected to result only from multiphoton processes, with no tunneling effect.

IV. CONCLUSION

A reliable tunable-wavelength mode-locked Nd-glass laser has been unsed to investigate for the first time the multiphoton ionization of rare gases on 10^{-11}-sec time scales. This work has emphasized several important points:

First, no resonance effects are observed in xenon, krypton, and argon atoms, although resonance conditions are satisfied for several atomic levels. It should be pointed out that resonance effects were observed in xenon and krypton atoms within the same wavelength and laser intensity range but for 10^{-8}-sec time scales. This absence of resonances is considered in terms of the short laser pulse duration (10^{-11} sec) with respect to the longer pulse duration (10^{-8} sec) in previous resonant multiphoton ionization experiments. Theoretical results appropriate to our experimental conditions do not as yet exist and are needed to investigate the influence of the laser pulse duration on resonant multiphoton ionization processes.

Secondly, the experiment was performed with both linearly and circularly polarized laser light. Linearly polarized laser pulses is found to be more efficient than the circularly polarized pulses,

in agreement with theoretical predictions.

Lastly, it is found that krypton can be ionized through the simultaneous absorption of 12 or 13 photons, depending on the laser wavelength selected within the tuning range of the Nd-glass oscillator. This experiment gives evidence of a lowering of 86 ± 6 cm^{-1} in the ionization energy of the krypton atom under the influence of the laser electric field of 1.2×10^8 V/cm.

ACKNOWLEDGMENTS

The authors wish to express their gratitude to Professor S. Feneuille, Dr. M. Trahin, and Dr. Y. Gontier for helpful theoretical discusssions. They are gratefully indebted to D. Fondant for assistance with the experiments.

[1]M. Lu Van, G. Mainfray, C. Manus, and I. I. Tugov, Phys. Rev. A 7, 91 (1973).
[2]G. A. Delone, N. B. Delone, and G. K. Piskova, Zh. Eksp. Teor. Fiz. 62, 1272 (1972) [Sov. Phys.-JETP 35, 672 (1972)].
[3]S. L. Chin, N. R. Isenor, and M. Young, Phys. Rev. 188, 7 (1969).
[4]M. Lambropoulos, S. E. Moody, S. J. Smith, and W. C. Lineberger, Phys. Rev. Lett. 35, 159 (1975).
[5]J. Bakos, A. Kiss, L. Szabo, and M. Tendler, Zh. Eksp. Teor. Fiz. Pis'ma Red. 18, 403 (1973) [JETP Lett. 18, 237 (1973)].
[6]G. Baravian, R. Benattar, J. Bretagne, G. Callede, J. L. Godart, and G. Sultana, Appl. Phys. Lett. 18, 387 (1971).
[7]D. Popescu, C. B. Collins, B. W. Johnson, and I. Popescu, Phys. Rev. A 9, 1182 (1974).
[8]E. H. A. Granneman and M. J. Van Der Wiel, J. Phys. B 8, 1617 (1975).
[9]J. L. Hall, IEEE J. Quantum Electron. QE-2, 361 (1966).
[10]R. A. Fox, R. M. Kogan, and E. J. Robinson, Phys. Rev. Lett. 26, 1416 (1971).
[11]R. Evans and P. Thoneman, Phys. Lett. 39A, 133 (1972).
[12]G. Brincourt, R. Caccioli, and Ch. Millet, Opt. Commun. 7, 384 (1973).
[13]M. R. Cervenan and N. R. Isenor, Opt. Commun. 13, 175 (1975).
[14]C. Lecompte, G. Mainfray, C. Manus, and F. Sanchez, Phys. Rev. A 11, 1009 (1975).
[15]T. U. Arslanbekov, Kvant. Electron. 3, 213 (1976) [Sov. J. Quant. Electron. 6, 117 (1976)].
[16]G. S. Agarwal, Phys. Rev. A 1, 1445 (1970).
[17]J. L. Debethune, Nuovo Cimento B 12, 101 (1972).
[18]F. Sanchez, Nuovo Cimento B 27, 305 (1975).
[19]L. Armstrong, P. Lambropoulos, and N. K. Rahman, Phys. Rev. Lett. 36, 952 (1976).
[20]J. Morellec, D. Normand, and G. Petite, Phys. Rev. A 14, 300 (1976).
[21]L. A. Lompre, G. Mainfray, C. Manus, S. Repoux, and J. Thebault, Phys. Rev. Lett. 36, 949 (1976).
[22]P. Agostini and C. Lecompte, Phys. Rev. Lett. 36, 1131 (1976).
[23]N. B. Delone, Usp. Fiz. Nauk. 115, 361 (1975) [Sov. Phys.-Usp. 18, 169 (1975)].
[24]B. Held, G. Mainfray, C. Manus, J. Morellec, and F. Sanchez, Phys. Rev. Lett. 30, 423 (1973).
[25]M. C. Richardson, IEEE J. Quantum Electron. QE-9, 768 (1973).
[26]L. A. Lompre, G. Mainfray, and J. Thebault, J. Appl. Phys. (to be published).
[27]L. A. Lompre, G. Mainfray, and J. Thebault, Appl. Phys. Lett. 26, 501 (1975).
[28]F. J. Holzrichter and D. R. Speck, J. Appl. Phys. 47, 2459 (1976).
[29]M. Crance and S. Feneuille, J. Phys. Lett. (Paris) 36, L235 (1976).
[30]P. Avan, C. Cohen-Tannoudji, J. Dupont-Roc, and A. Fabre, J. Phys. (Paris) 37, 993 (1976).
[31]P. Lambropoulos, Phys. Rev. Lett. 28, 585 (1972).
[32]Y. Gontier and M. Trahin, Phys. Rev. A 7, 2069 (1973).
[33]L. V. Keldysh, Zh. Eksp. Teor. Fiz. 47, 1945 (1964) [Sov. Phys.-JETP 20, 1307 (1965)].